Geometric structure and chemical composition of SrTiO₃ surfaces heated under oxidizing and reducing conditions

A. Gunhold [a,*], K. Gömann [b], L. Beuermann [a], M. Frerichs [a], G. Borchardt [b], V. Kempter [a], W. Maus-Friedrichs [a]

[a] *Institut für Physik und Physikalische Technologien, Technische Universität Clausthal, Leibnizstraße 4, D-38678 Clausthal-Zellerfeld, Germany*
[b] *Institut für Metallurgie, Technische Universität Clausthal, Robert-Koch-Strasse 42, D-38678 Clausthal-Zellerfeld, Germany*

Abstract

SrTiO₃(1 0 0) single crystals with two different donor dopant concentrations were heated at 1300 °C in synthetic air and ultrahigh vacuum, respectively, and afterwards studied with atomic force microscopy to characterize the surface topology. Depth profiling measurements utilizing Auger electron spectroscopy yielded information on the chemical composition of secondary phases forming on top of the surface during annealing and of the surface region between them. Under oxidizing conditions a formation of SrO_x insulating islands appearing on top of the surface is observed which strongly depends on crystal doping. Between these islands the formation of an additional phase is found. In contrast to the air heated surfaces no material enrichment and no SrO_x formation is found under reducing conditions. © 2002 Elsevier Science B.V. All rights reserved.

Keywords: Alkaline earth metals; Titanium oxide; Surface structure, morphology, roughness, and topography; Diffusion and migration; Atomic force microscopy; Auger electron spectroscopy

1. Introduction

Strontium titanate (SrTiO₃) has been extensively investigated because of its suitability as perovskite model substance and for technological applications, such as resistive high temperature oxygen sensors. In numerous studies (see Refs. [1–3], for example, and references therein) the electronic structure and the topography of the stoichiometric surface [4–6] and the influence of different types of defects [7,8] were examined.

Thermal treatment of SrTiO₃ causes a restructuring of the surface region leading to increasing chemical heterogeneity [9], a broad range of new topographical features like ridges [10] or step terrace structures [2,11] and a formation of secondary phases on top of the surface [2,3,12–14], thus affecting the sensor characteristics of the material. The observed phenomena are considered to depend on kind and concentration of the dopant and on atmosphere and temperature of the annealing procedure but, according to Szot et al. [3], do not necessarily follow the point defect chemical predictions (for the bulk). Whereas in acceptor doped SrTiO₃ only the anion sublattice is interacting with the ambient atmosphere (see Ref. [15], for example), oxidation of donor doped SrTiO₃ leads

* Corresponding author. Tel.: +49-5323-722756; fax: +49-5323-723600.

E-mail address: anissa.gunhold@tu-clausthal.de (A. Gunhold).

to the formation of strontium vacancies [17]. The excess strontium might be contained in layered Ruddlesden–Popper (RP) phases (SrO · nSrTiO$_3$) within the crystal [14] or it migrates to the surface where it forms crystallographically ordered SrO$_x$ phases [12–14] and in part even evaporates [3]. Alternatively, at temperatures below 1100 °C and donor dopant concentrations below 1 at.% also TiO$_x$-needles on the surface were reported.

We present atomic force microscopy (AFM) and Auger electron spectroscopy (AES) data of La-doped SrTiO$_3$(1 0 0) single crystals that were heated not only in air, but also in ultrahigh vacuum to better understand the influence of dopant concentration and ambient oxygen partial pressure (pO$_2$) on the above processes in donor doped SrTiO$_3$.

2. Experimental

Polished SrTiO$_3$(1 0 0)-oriented single crystals with two different lanthanum dopant concentrations (5 and 0.1 at.%) were obtained from CrysTec, Berlin. The crystals were grown under reducing conditions. During these investigations the crystals were heated at 1300 °C in ultrahigh vacuum (UHV, base pressure $\sim$10^{-10} mbar) and in synthetic air (20% O$_2$ and 80% N$_2$), respectively.

The samples were analysed after 2 and 25 h thermal treatment with AFM and AES. The chemical composition was studied by an Auger microprobe (PEM 595). An argon ion gun was applied for sputtering to obtain a depth profile. The concentration profiles were calculated from AES peak to peak ratios, and from the respective sputtering rate. Sensitivity factors normalised to the bulk composition of a stoichiometric SrTiO$_3$ were used to calculate the atomic concentrations of the main components in the chemical compound. For the microscopic measurements an Omicron UHV AFM/STM was used.

3. Results and discussion

3.1. Microscopic investigations

Fig. 1(A) shows the AFM image of the surface of a 5 at.% La-doped sample after 25 h thermal
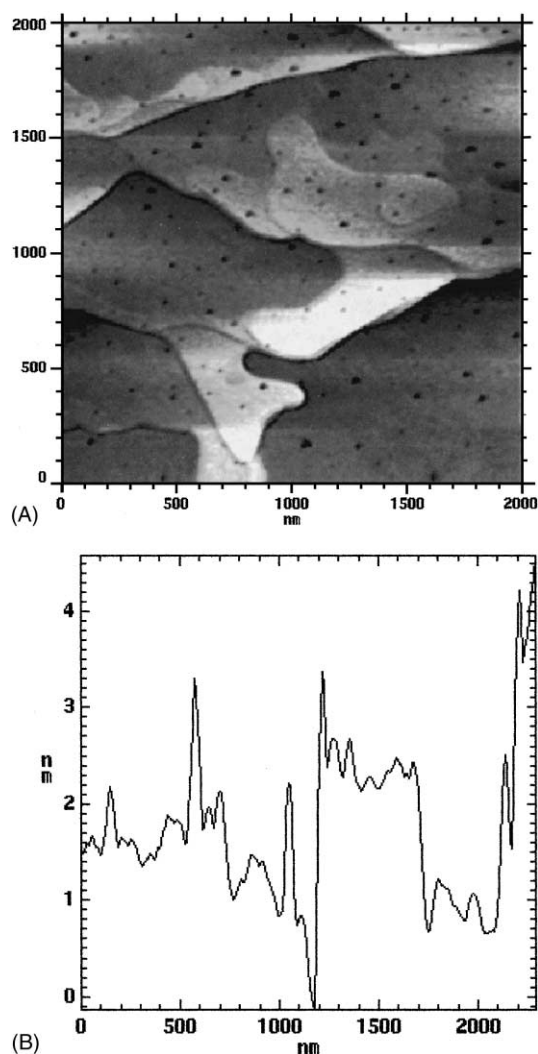

Fig. 1. (A) AFM analysis of the SrTiO$_3$ single crystal doped with 5 at.% La and heated for 25 h in synthetic air (visible area 2 × 2 μm^2), (B) corresponding line profile.

treatment in synthetic air. We concentrate on areas between the large number or SrO$_x$ crystals grown during this treatment, which have been described in detail previously [3,13]. Due to the heating procedure disordered ridges and terraces form on top of the surface between the islands. The observed step heights (Fig. 1(B)) typically correspond to 12, 20 and 28 Å, which may be assigned to RP phases (Sr$_{n+1}$Ti$_n$O$_{3n+1}$, n = 1, 2 or 3) [3,18,19]. These step heights can be found all over the sur-

face between the microcrystals. On top of the surface, irregular holes could be found. These holes are typically about several tens of nanometers wide. They are assumed to be due to a desorption process.

In contrast, the 5 at.% La-doped sample annealed 25 h in UHV does not show changes in surface topography or formation of secondary phases (Fig. 2(A)). The step heights (Fig. 2(B)) are still found to be about 4 Å, which corresponds well with the step height of $SrTiO_3$ in [0 0 1] direction [20]. Like on the sample annealed in synthetic air on top of the surface rectangular, obviously crystallographically oriented holes appear with edge lengths up to 50 nm. This may equally be explained with a desorption process. Additional AES measurements did not reveal any change in the chemical composition of the surface during heat treatment.

After 2 h thermal treatment on the surface of the 0.1 at.% La-doped specimen a terrace-like topography with microcrystals is observed, but no SrO_x crystals are formed (AFM image is not shown here). After annealing for 25 h the microcrystals have vanished and the terrace structures develop crystallographically oriented right-angle steps (Fig. 3(A)) with typical step heights of about 12 Å (Fig. 3(B)), which may also be assigned to a RP (with $n = 1$) phase. No further precipitates could be observed.

In contrast to the strongly doped sample, the 0.1 at.% La-doped sample annealed for 25 h in UHV does show changes in surface topography and the formation of secondary phases (Fig. 4(A)). The typical step heights of 3.3 and 6.6 Å (Fig. 4(B)) may be assigned to Ti_xO_y phases (Magneli phases). Also, no holes were found on top of the surface.

3.2. Spectroscopic investigations

The chemical composition of the surface and the subsurface region was investigated by Auger depth profiling. Fig. 5 shows the concentration profiles of the 5 at.% La-doped $SrTiO_3$ heated in synthetic air. On the surface a depletion of Sr and Ti and an enrichment of O and La could be observed. In the subsurface region the Sr concentration is about 30% higher than in the unheated
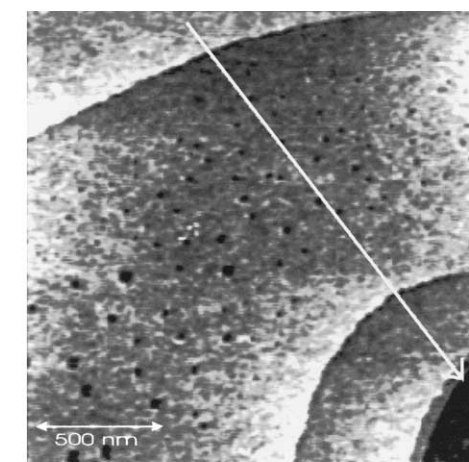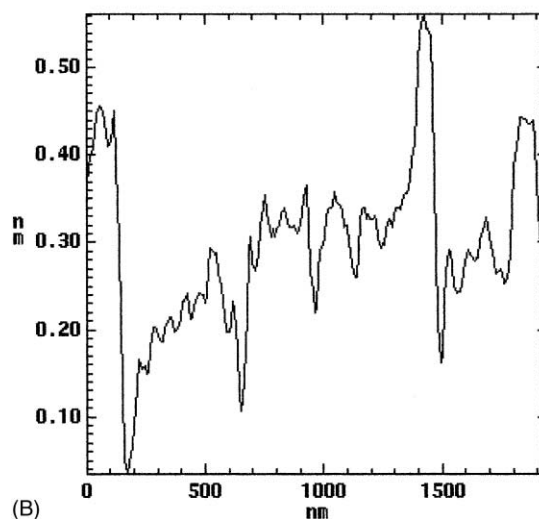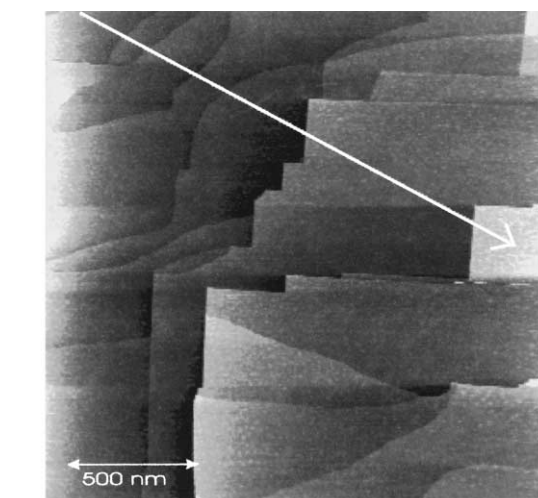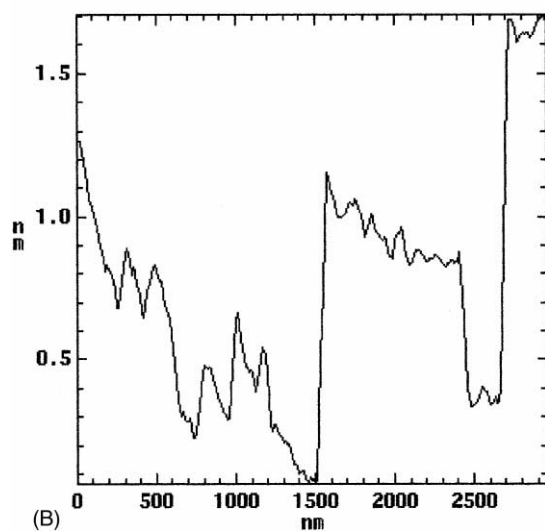

Fig. 2. (A) AFM image of the $SrTiO_3$ single crystal doped with 5 at.% La and heated for 25 h in UHV (visible area 2×2 μm^2). The white arrow indicates the position of the line profile, (B) corresponding line profile.

crystal (dotted line) and reaches the value of the unheated crystal after about 3 nm sputtering. The Ti concentration in the subsurface region (0.5–1.5 nm) is about 15% higher than in the unheated $SrTiO_3$ and decreases after 2 nm sputtering below the value of the unheated crystal and reaches it after 5 nm sputtering. The O concentration in the subsurface region is about 15% lower than in the unheated crystal and reaches the bulk value after about 2.5 nm sputtering. The La concentration
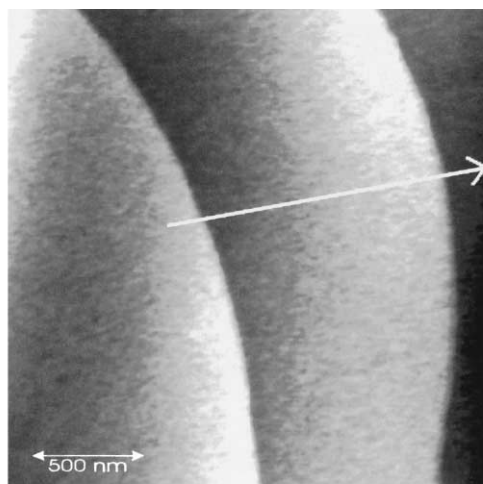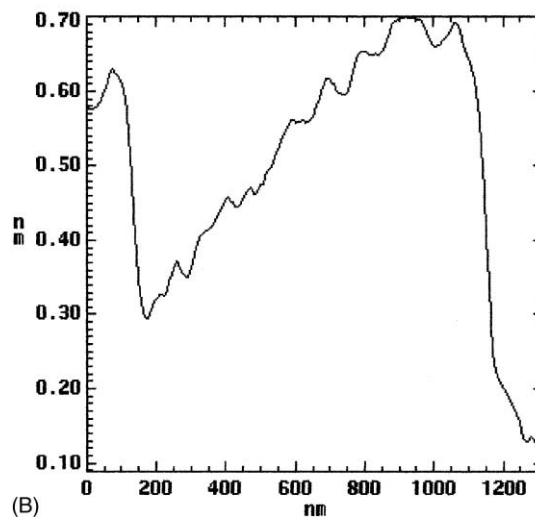
(A)

(B)

Fig. 3. (A) AFM analysis of the SrTiO$_3$ single crystal doped with 0.1 at.% La and heated for 25 h in synthetic air (visible area 2 × 2 μm^2). The white arrow indicates the position of the line profile, (B) corresponding line profile.

reaches the value of the unheated SrTiO$_3$ after about 1 nm sputtering. The high O concentration on top is not understood up to now.

The depth profiles of the 0.1 at.% La-doped SrTiO$_3$ crystal shown in Fig. 6 also indicate an enrichment of O and a depletion of Sr and Ti at the surface, but the depletion of Sr is more evident compared to Ti. This supports the picture of Magneli phase formation suggested above. The O

(A)

(B)

Fig. 4. (A) AFM analysis of the SrTiO$_3$ single crystal doped with 0.1 at.% La and heated for 25 h in UHV (visible area 2 × 2 μm^2). The white arrow indicates the position of the line profile, (B) corresponding line profile.

concentration reaches the value of the unheated crystal after 0.5 nm sputtering. The Sr and Ti concentrations reach the value of the unheated crystal after about 5 nm sputtering.

4. Summary

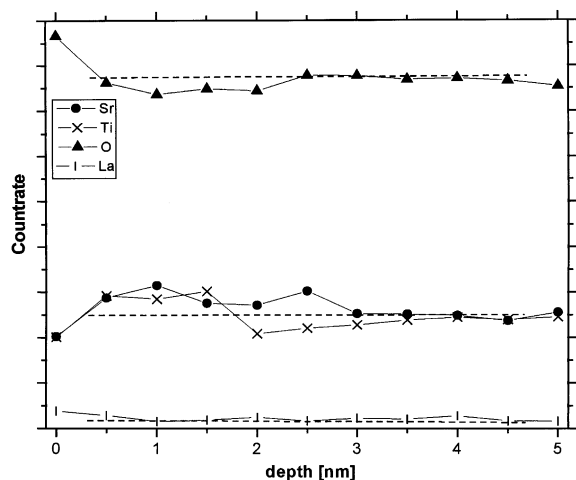5 at.% La-doped SrTiO$_3$(1 0 0) single crystals heated in air develop terrace structures at the

Fig. 5. AES depth profile of the 5 at.% La-doped SrTiO$_3$(1 0 0) single crystal heated for 25 h under oxidizing conditions. The dashed lines indicate the countrate of the untreated stoichiometric crystal, respectively.

Fig. 6. AES depth profile of the 0.1 at.% La-doped SrTiO$_3$(1 0 0) single crystal heated for 25 h under oxidizing conditions. The dashed lines indicate the countrate of the untreated stoichiometric crystal, respectively.
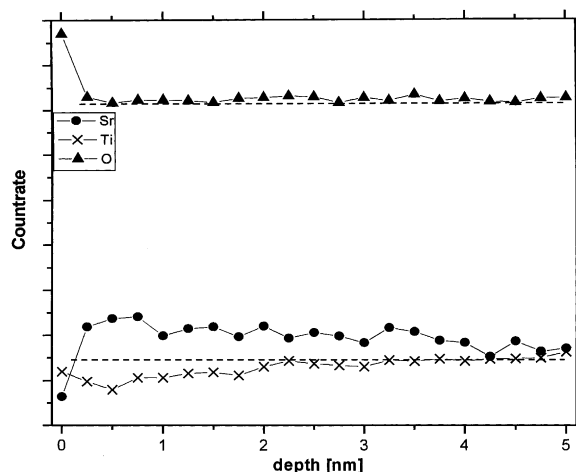
surface between the well observed formation of large SrO$_x$ islands. These structures show step heights that may be assigned to RP-phases (Sr$_{n+1}$-Ti$_n$O$_{3n+1}$) reaching from $n = 1$ to 3. On top of these phases an additional oxygen enrichment is found being not understood up to now. Also observed is the enrichment of La on the surface. Heating of

similar crystals under reducing conditions in vacuum does not change the geometric structure and the chemical composition of the surface.

Although 0.1%-doped SrTiO$_3$ surfaces heated in air do not show the formation of SrO$_x$ islands, terrace structures appear that may also be connected to the formation of RP phases. Similar to the 5%-doped crystal an oxygen enrichment on the surface occurs being not yet understood. In contrast to this, on 0.1 at.% La-doped crystals annealed in UHV the formation of a secondary phase with typical step heights of 3.3 and 6.6 Å is observed together with a relative Ti enrichment thus leading to the picture of the formation of a Ti$_x$O$_y$ rich phase (possibly a Magneli phase).

The formation of secondary SrO$_x$ crystals and RP phases and the corresponding Sr enrichment at the surface during heating in air can be explained by the bulk defect chemistry model for donor doped SrTiO$_3$ [16]. The crystals, being produced under reducing conditions, are oxidized during annealing. Thus the concentration of oxygen vacancies and dislocated electrons is strongly reduced and the donor dopant compensation mechanism changes to Sr vacancy compensation leading to a diffusion of Sr vacancies into the crystal. The excess Sr accumulates at the surface forming RP phases at low dopant concentrations (0.1 at.% La). The larger amount of excess Sr at high dopant concentrations (5 at.% La) results in the additional formation of secondary SrO$_x$ phases on top of the surface. In contrast, annealing in UHV further reduces the crystal surface leading to the observed holes and possibly also Magneli-phases by reducing Ti^{4+} partly to Ti^{3+}. The model does however not explain the observed O and La enrichment at the surface and the behaviour of Sr and Ti in the subsurface region confirming the findings of Szot et al. [3], that present bulk defect chemistry models are not sufficient to understand the processes occuring at the surface and in the surface near region during annealing.

References

[1] V.E. Henrich, P.A. Cox, The Surface Science of Metal Oxides, Cambridge University Press, Cambridge, England, 1994.

[2] K. Szot, W. Speier, Phys. Rev. B 60 (1999) 5909.

[3] K. Szot, W. Speier, U. Breuer, R. Meyer, J. Szade, R. Waser, Surf. Sci. 460 (2000) 112.

[4] M.F. de Groot, J. Faber, J.J. Michiels, M.T. Czyzyk, M. Abbate, J.C. Fuggle, Phys. Rev. B 48 (1993) 2074.

[5] O.V. Krasovska, E.E. Krasovskii, V.N. Antonov, Solid State Commun. 97 (1996) 1019.

[6] H. Haruyama, S. Kodeira, Y. Aiura, H. Bando, Y. Nishihara, T. Maruyama, Y. Sakisaka, H. Kato, Phys. Rev. B 53 (1996) 8032.

[7] V.E. Henrich, Prog. Surf. Sci. 14 (1983) 175.

[8] J. Noffke, H. Wern, R. Heise, Phys. Rev. B 42 (1990) 9127.

[9] K. Szot, W. Speier, J. Herion, Ch. Freiburg, Appl. Phys. A 64 (1997) 55.

[10] S.S. Sheiko, M. Möller, E.M.C.M. Reuvekamp, H.W. Zandbergen, Phys. Rev. B 48 (1993) 5675.

[11] B. Stäuble-Pümpin, B. Ilge, V.C. Matijasevic, P.M.L.O. Scholte, A.J. Steinfort, F. Tuinstra, Surf. Sci. 369 (1996) 313.

[12] Y. Liang, D.A. Bonnell, Surf. Sci. 310 (1994) 128.

[13] H. Wei, L. Beuermann, J. Helmbold, G. Borchardt, V. Kempter, G. Lilienkamp, W. Maus-Friedrichs, J. Euro. Ceram. Soc. 21 (2001) 10.

[14] R. Meyer, K. Szot, R. Waser, Ferroelectrics 224 (1999) 751.

[15] R. Waser, J. Am. Ceram. Soc. 74 (1991) 1934.

[16] R. Moos, K.-H. Härdtl, J. Amer. Ceram. Soc. 80 (1997) 2549.

[17] M. Frerichs, A. Gunhold, W. Maus-Friedrichs, V. Kempter, Surf. Sci. 488 (2001) 239.

[18] S.N. Ruddlesden, P. Popper, Acta Crystallogr. 10 (1957) 538.

[19] S.N. Ruddlesden, P. Popper, Acta Crystallogr. 11 (1958) 54.

[20] R.W.G. Wyckoff, Crystal Structures, John Wiley & Sons, New York, 1963.